Supplementary Materials for

Sustainable greenhouse production with transparent radiative cooling film

Hao Zou, Chenxi Wang, Jiaqi Yu, Danfeng Huang*, Ronggui Yang*, Ruzhu Wang*
Correspondence to: rzwang@sjtu.edu.cn (R.Z.W.); hdf@sjtu.edu.cn (D.F.H.);
ronggui@hust.edu.cn (R.G.Y.).

This PDF file includes:

Materials and Methods
Supplementary Text
Figs. S1 to S10
Tables S1 to S2

Materials and Methods

Fabrication of T-RC film.

The T-RC film was prepared using the following process. Two silver layers with thickness of tens nanometer were first coated on polyethylene terephthalate (PET) to induce optical selective reflectance in UV and NIR range. And then a visibly transparent polymer film with C-F bonds was used to cover the silver layers to form a optical selective emitting layer. The total thickness of the T-RC film is about 115 μm.

Measurement of environmental indicators.

We deploy different sensors to measure the temperature on the film, soil temperature and indoor and outdoor temperature and humidity, light and irradiation. During the experiment period, three thermocouples (K type, Omega) were hanging in the front, middle and back of each greenhouse to measure the indoor temperature. A thermocouple was buried in soil at depth of 2 cm at the same place for each greenhouse to monitor the temperature evolution. Another thermocouple was taped to the backside of the film to get the film temperature. For every thermocouple under the sunlight, a little piece of aluminum foil was used to shield the measurement point from direct solar irradiation. All thermocouples were pre-calibrated using a thermostatic water tank to ensure an accuracy of 0.2 ^{o}C in the interested temperature range. The horizontal incident solar irradiation and PAR was recorded using a pyranometer (JTBQ-2, JinZhou TINEL, Inc.) with a directional response of less than $50W/m^2$. Other external meteorological conditions, including ambient temperature and wind velocity, was measured with a portable weather station at the experimental site. All measurement signals were logged by a data acquisition center (34972A, Agilent, Inc) in every 10 seconds.

Cultivation of three indicator crops.

We choose Chinese cabbage, Pakchoi, and cherry radish for the trial because all three crops are summer staples in greenhouses in the middle and lower reaches of the Yangtze River region. Those three different crops were chosen for the experiment to observe the magnitude of the effects of T-RC films on different crops. These three crops differed greatly in leaf area, leaf sparseness, and above-ground to below-ground ratios, allowing for a more visual representation of how different types of crops respond to T-RC films. The three indicator crops were sown directly into the soil in two identical greenhouses covered with T-RC film and PO film at Shanghai Sunqiao Yijia Agricultural Technology Co., Ltd (31.19°N, 121.70°E). The plastic greenhouse selected for the experiment was 15 m long and spanned 8 m, and was evenly divided into 3 × 3 plots of 3.8 m length and 2.2 m width. We controlled the number of seeds sown in each plot to be the same to eliminate the initial experiment error. The seeds were sown by scattering, 16.7 g per plot for cherry radish, 13.3 g per plot for Chinese cabbage and 5 g per plot for Pakchoi. Drip irrigation was used for watering in each plot and the same time and total water consumption was ensured for each watering in both greenhouses. The plants were irrigated as needed (every 2–3 d) with reverse-osmosis water supplemented with the same water-soluble fertilizer that supplied the following nutrients (in g m-3): 100 N, 60 P, 400 K, 150 Ca, 50 Mg, 50 S, 0.5 Fe, 0.3 Mn, 0.3 Zn, 0.5 B, 0.5 Cu and 0.5 Mo. The electrical conductivity (EC) ranged from 1.8 to 2.0 mS cm^{-1} and the pH of the as-prepared solutions was routinely adjusted to 6.5–6.8 using potassium bicarbonate.

Physiological and biochemical parameters of crops.

From the date of treatment, morphological indexes were measured by destructive sampling. We took four samples of plants in each plot randomly for each measurement. Plant height (the distance from the base of the plant to the highest part of the top), maximum leaf length and leaf width were measured for each treatment. For the cherry radish, we also measured the length and width of the lower part of the ground. After harvesting, four samples of plants in each plot were locally controlled and randomly selected to measure their above-ground and below-ground fresh and dry weights (dried in a drying oven at 65°C until the mass was constant). The harvesting of all crops was done at once during the harvesting period, the total biomass (gross weight of hairy vegetables), total numbers and single plant weight were measured. Net vegetable is obtained by uniformly removing the outer layer of leaves from the hairy vegetables. We also did crop quality measurement. The soluble sugar, proline, chlorophyll and cellulose contents of net vegetables were measured by sampling at the same time of harvesting. The measurement of the four quality indicators was done by enzyme labeling method.

Statistical analysis.

All of the bar and line chart plots were processed and drawn using Origin 2021 of education edition (Origin Lab). Analysis of variance (ANOVA) followed by the least significant difference (LSD) test at a significance threshold of 5% and 1% was performed using SPSS 23.0 software (IBM) and EXCEL 2019 to determine the significance for the experiments. Multiple comparisons were performed using Duncan's new complex polarization method.

Supplementary Text

Greenhouse ventilation operation

It should be noted that the experiment went through two stages totally: initially, the two greenhouses were completely closed, and the side ventilation of the two greenhouses was opened on the evening of August 11, the later measurements were made under natural ventilation.

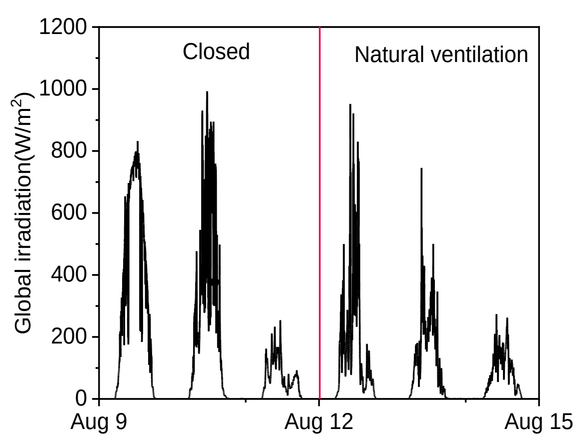

Fig. S1. Global irradiation of two greenhouses under closed and natural ventilation conditions.

Indoor temperature difference between greenhouses throughout the reproductive cycle under natural ventilation.

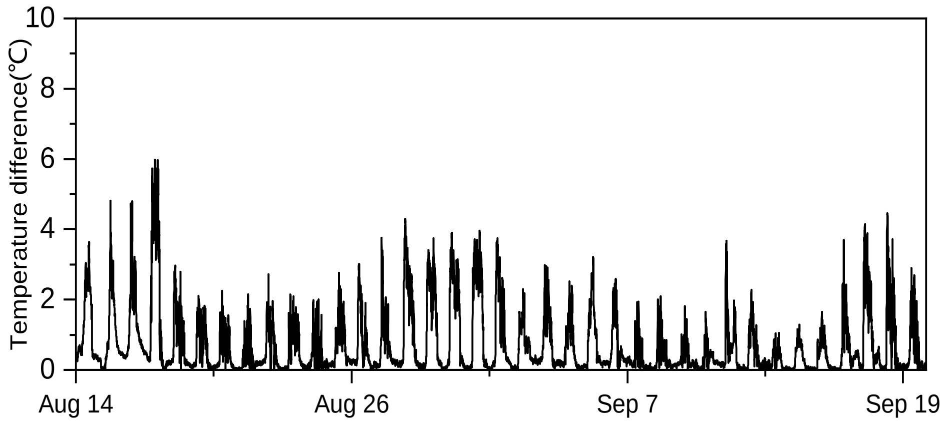

Fig. S2. Global irradiation of two greenhouses under closed and natural ventilation conditions.

Germination rate of three crops

We did statistics on the germination potential and germination rate of the three crops on the third and seventh days after sowing. For all kinds of crops, the germination rate and potential of experimental greenhouse were obviously higher than that of control greenhouse.

Fig. S3. Comparative photographs of experimental and control greenhouse germination rates.

Table S1. Germination potential and germination rates of three different crops

Crops		Germination potential	Germination rates
Cherry radish	Control	30.73%	56.66%
	Experiment	50.90%	84.51%
Chinese cabbage	Control	50.40%	69.07%
	Experiment	69.60%	92.27%
Pakchoi	Control	38.08%	61.76%
	Experiment	61.44%	84.80%

Leaf length and width of three crops in the whole growth cycle

In the final stages, the growth was slowed down in the experiment greenhouse due to the shading effect caused by the lack of space between each plant during the continuous expansion and growth of the leaves. This is due to more plants germinated normally in experiment greenhouse in the germination stage, and more crops means less space for each crop to survive. In contrast, the control greenhouse had fewer germinating plants, which did not shade each other. The plants grew normally, resulting in the leaves of the two leafy vegetables in the control greenhouse being larger than those in the experiment greenhouse in the end. However, it should be noted that the last indicator collection was well after the normal harvest time, and the actual normal harvest time would have been at the penultimate harvest. The reason for harvesting a week late was to further investigate the effect of T-RC film on the end part of crop growth. Meanwhile, the cabbages in the control greenhouse had not yet reached harvesting standards by the penultimate harvest. As the leaves of cherry radish were sparse, the shading effect was not obvious even in the late stage of growth. All the nutritional growth indexes of cherry radish were higher in the experimental greenhouse than in the control greenhouse throughout the reproductive stage, which showed that the T-RC film had a great effect on the advancement of its reproductive stage and the improvement of its nutritional growth.

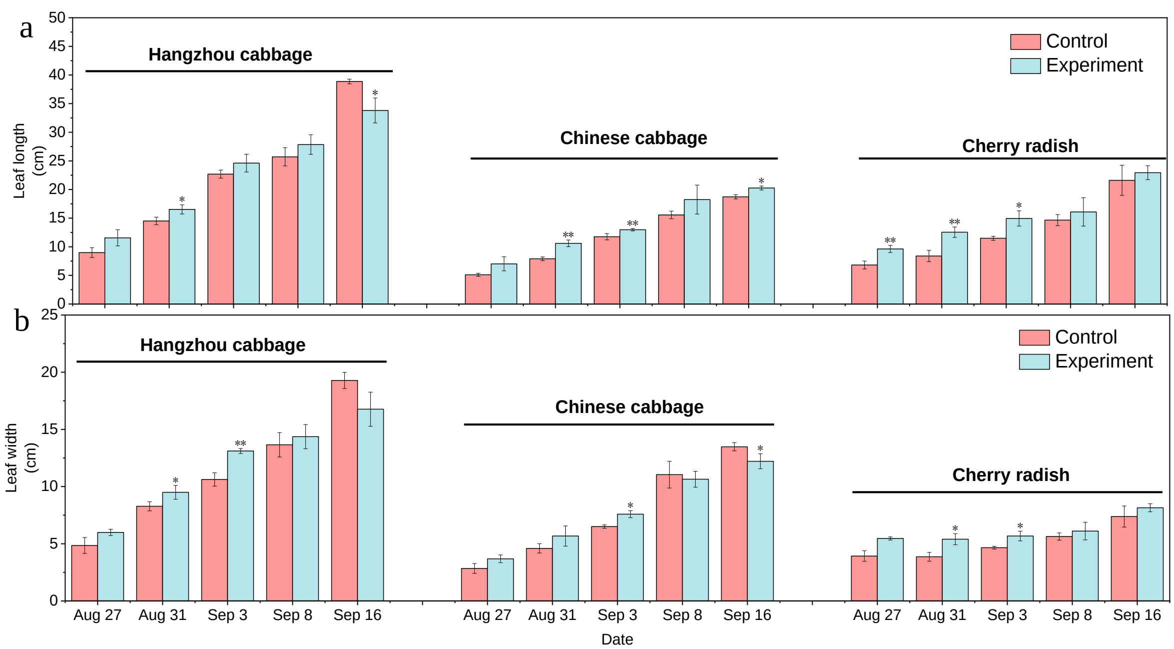

Fig. S4. Leaf length(a), leaf width(b) of three indicator crops during the entire reproductive cycle from full germination.

Fresh and dry weight of three crops

The cherry radishes in the experiment greenhouse were significantly heavier than those in the control greenhouse, both above and below ground. The accumulation of dry matter mass showed the same trend. Differences in nutrient organs and equivalent yield were as high as 76.2%±2.8% and 120.1%±5.9%, respectively. In contrast, for Chinese cabbage and Pakchoi, the fresh and dry weights of individual plants were lighter in the experimental greenhouse than in the control greenhouse due to the sheltered reaction mentioned in the main text. However, because the number of plants in the experiment greenhouse was much higher than that in the control greenhouse, the equivalent yields of leafy vegetables in both greenhouses were essentially the same . It should also be noted that these yields were measured at the very final stage of growth, which actually exceeded the normal growth frame of leafy greens in the experiment greenhouse. If the measurement time was predicated by one week to the normal harvesting time of leafy greens in the experiment greenhouse, the dry and fresh weights, and the equivalent yield of leafy greens in the experiment greenhouse would be much higher than those in the control greenhouse. It is evidenced by the fact that the yield of cherry radish in the experimental greenhouse was extremely significantly higher than that in the control greenhouse.

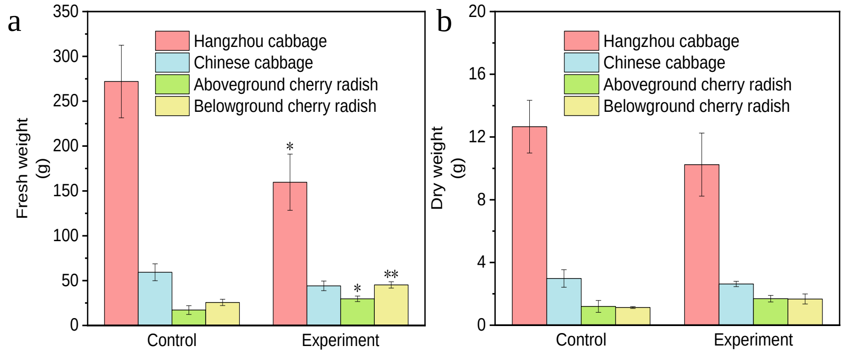

Fig. S5. Fresh weight(a), dry weight(b) of three indicator crops at day 30 after sowing in experimental and control greenhouse.

<u>Chlorophyll of three crops</u>

The chlorophyll a, b and total content of the three crops showed that when covering the T-RC film, although the indoor light quality is changed, the chlorophyll accumulation and the photosynthetic metabolism for crops had been less influenced.

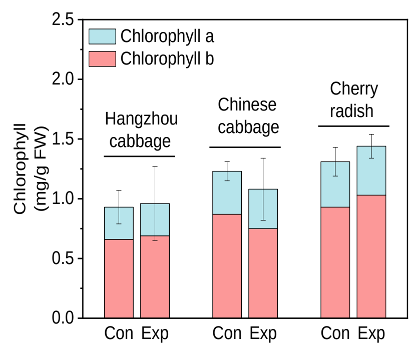

Fig. S6. Chlorophyll of three indicator crops at day 30 after sowing in experimental and control greenhouse.

<u>Details of the simulation method</u>

A simulation model based on mass and energy conversation was developed here to understand and predict the interactions between covering materials, indoor air, crops, and other components in the greenhouse. In past studies, microclimate models can be classified into static and dynamic ones. In the static models, the heat storage capacities of all greenhouse components are neglected, which ignores the time lag between these components and the outside environment. Hence, a dynamic model is chosen in this work to better predict the temperature variations in the greenhouse. Besides, a crop yield model was integrated with the climate model to describe the effects of greenhouse climate on yield.

Some basic assumptions of this model read as follows:

1. The greenhouse is assumed to a perfectly stirred tank, which means uniform temperature, moist, and carbon oxide content in the greenhouse.
2. Inside air dose not participate in the radiation exchange process.
3. The mass and energy exchanges between the crops and inside air are described by treating the canopy layer as a 'big leaf'.

Notational conventions Subhead

All state variables and fluxes involved in the model are denoted by their subscripts, taking the naming conventions in the work of De Zwart(*1*) and Vanthoor et al.(*2*) as reference. Specifically, state variables are distinguished by their capital letters, i.e. T for temperature, C for heat capacity. The single subscript following the state variable capital denotes the consideration object (i.e. T_{air}). Fluxes are characterized by capital letters followed by two subscripts, with the first one representing the source and the second one representing the sink of the fluxes.

Conversation equations in the model

For covering material:

$$A_{cover}C_{cover}\frac{dT_{cover}}{dt} = H_{air-cover} - H_{cover-out} + L_{air-cover} + QS_{cover} - QR_{cover-floor} - QR_{cover-canopy} - QR_{cover-sky}$$

where C_{cover} is the heat capacity of the covering materials. The temperature variation of the covering is determined by the sensible heat exchange between the covering materials and other elements, i.e. inside air ($H_{air-cover}$) and outside air ($H_{cover-out}$), the latent heat exchange with inside air ($L_{air-cover}$), absorbed solar irradiation (QS_{cover}), longwave radiational heat exchange between cover and floor ($QR_{cover-floor}$), canopy $QR_{cover-canopy}$, sky($QR_{cover-sky}$).

For indoor air:

$$C_{air}V\frac{dT_{air}}{dt} = H_{floor-air} + H_{veg-air} - H_{air-cover} - H_{air-out} + QS_{air}$$

Where C_{air} is the volumetric capacity of the indoor air, V is the volume of the greenhouse. Sensible heat is exchanged between the indoor air and other greenhouse elements, namely the floor($H_{floor-air}$), the canopy layer($H_{veg-air}$), the covering materials ($H_{air-cover}$). Moreover, part of sensible energy is exchanged between the indoor air and external environment ($H_{air-out}$) due to air exchange, including air leakage, natural ventilation and forced ventilation. QS_{air} refers to the solar irradiation which is absorbed by the greenhouse structure elements and is assumed to be directly released to the indoor air.

For canopy layer,

$$C_{canopy}A_{canopy}\frac{dT_{canopy}}{dt} = QS_{canopyNIR} + QS_{canopyPAR} - H_{canopy-air} - L_{canopy-air} + QR_{cover-canopy} - QR_{canopy-floor} - QR_{canopy-sky}$$

Where C_{canopy} is the heat capacity of the crop leaf, A_{canopy} is the leaf area on unit floor area, namely leaf area index(LAI), $QS_{canopyNIR}$ is the NIR part of global irradiation absorbed by the canopy, $QS_{canopyPAR}$ is the PAR part absorbed by the canopy. $H_{canopy-air}$, $L_{canopy-air}$ is the sensible and latent heat exchange between the canopy and the indoor air, respectively. Longwave radiation is exchanged between the canopy and the cover, $QR_{cover-canopy}$, the floor, $QR_{canopy-floor}$, and the sky, $QR_{canopy-sky}$.

The mass conversation equation of vapor inside the greenhouse is given as:

$$V\frac{dC_{vapor}}{dt} = (L_{canopy-air} + L_{floor-air} - L_{air-cover} - L_{air-out}) / \lambda_{eva}$$

Where C_{vapor} is the absolute humidity of the indoor air, $L_{air-out}$ is the latent heat loss due to air exchange, including air leakage, natural ventilation and forced ventilation. λ_{eva} is the vaporization heat of water.

The mass conversation equation of carbon oxide inside the greenhouse is given as:

$$V\frac{dC_{CO2}}{dt} = -MC_{air-out} + (MC_{buf-air} + MC_{fruit-air} + MC_{stem-air} + MC_{leaf-air}).A_v.(\frac{M_{CO2}}{M_{carbohydrate}})$$

Where C_{CO2} is the content of carbon oxide of the indoor air, $MC_{air-out}$ is the carbon exchange rate with the outside air due to air leakage, natural ventilation and forced ventilation. $MC_{buf-air}$ is the growth respiration of the total plant per unit area of cultivate floor, $MC_{fruit-air}, MC_{stem-air}, MC_{leaf-air}$ is the maintenance respiration of the individual plant organs per unit area of cultivate floor, A_v is the cultivated floor area inside the greenhouse, $\frac{M_{CO2}}{M_{carbohydrate}}$ is the conversion factor from carbohydrate (CH_2O) to carbon oxide. The carbohydrate flow listed above will be determined in the crop growth model.

Fluxes calculation

1 Convective heat transfer calculation

The universal form of convective heat flux between object 1 and object 2 can be written as following:

$$H_{12} = h_{12}(T_1 - T_2)$$

Where h_{12} denotes the heat exchange coefficient between the two objects. Hence, the key of calculating convective heat flux falls on determining the accurate heat exchange coefficient. Considering the complex condition in the greenhouse, a criterion has to be defined for identifying the convective mode (free convection or forced convection) and the type of flow state (laminar flow or turbulent flow). The dimensionless number Ri, is recommended as the criterion to distinguish free or forced convention. Furthermore, the criterion of flow state is Gr in the case of free convection and Re in the case of forced convection. The empirical formulates used in determining heat transfer coefficients inside the greenhouse are listed in the Table S1.

Table S2. Empirical formulates used in determining heat transfer coefficients(3)

Flow type	Laminar flow	Turbulent flow
Free convection (Ri<0.1)	$Nu_{free} = 0.54(Gr.\mathrm{Pr})^{1/4}$	$Nu_{free} = 0.14(Gr.\mathrm{Pr})^{1/3}$

Forced convection (Ri>15)	$Nu_{forced} = 0.67\,\mathrm{Re}^{1/2}\,\mathrm{Pr}^{1/3}$	$Nu_{forced} = 0.036\,\mathrm{Re}^{4/5}\,\mathrm{Pr}^{1/3}$
Mixed Convection (1⩽Ri ⩽15)	$Nu^{7/2} = Nu_{forced}^{7/2} + Nu_{free}^{7/2}$	

2 Latent heat transfer calculation

The latent heat transfer between a solid surface and the flow air is determined by the analogy relationship between the heat and mass transfer, reads as:

$$Sh = Nu.Le^{m}$$

Where Sh is the dimensionless Sherwood number, Nu is the Nusselt number determined in the last section, Le is the Lewis number for vapor. The power coefficient m equals 0.25 for laminar condition and 0.33 for turbulent condition, respectively.

Then, the mass transfer coefficient can be determined as:

$$h_m = Sh.D / \mathrm{L}$$

Where h_m is the mass transfer coefficient, D is the vapor diffusivity in air, L is the characteristic length of the soil surface.

The latent heat flux is described in a form analogy to the sensible heat flux, shown as:

$$\mathrm{L}_{12} = h_{m12}(C_{vapor1} - C_{vapor2})$$

Where L_{12} is the latent heat flux from object 1 to object 2, h_{m12} is the corresponding mass transfer coefficient, $(C_{vapor1} - C_{vapor2})$ is the absolute moist content difference between the two objects which work as the driving force of the mass transfer process.

3 Solar irradiation

Solar irradiation is the main energy resource of the passive greenhouse and plays an important role in the energy balance of the indoor climate. The solar radiation can be split to three different wavelength bands, namely UV light (0.3-0.4um), visible light (PAR, 0.4-0.7um), and the near infrared light (NIR, 0.7-2.5um). For the sake of simplicity, in the model 50% of the total solar energy is assigned to the visible part and the other 50% is attributed to the NIR part.

Considering the canopy is composed of a series of stratified layers, the light entering the canopy will go through several times of transmissions and reflections within the canopy. We chose the empirical formulas proposed by De Zwart(*1*) to compute the absorption of the canopy layer. Specific formulas are listed as follows:

$$\alpha_{canopy\_fVIS} = 0.95 - 0.9\exp(-k_{fVIS}.LAI)$$

$$\alpha_{canopy\_rVIS} = 0.94 - 0.95\exp(-k_{rVIS}.LAI)$$

$$\alpha_{canopy\_fNIR} = 0.65 - 0.65\exp(-k_{fNIR}.LAI)$$

$$\alpha_{canopy\_rNIR} = a - b\exp(-k_{rNIR}.LAI)$$

$$a = 0.67 - 0.36\exp(-0.095\beta)$$

$$b = 0.68 - 0.50\exp(-0.11\beta)$$

where subscript $fVIS$ and $rVIS$ denotes diffuse visible light and direct light part in the global irradiation, $fNIR$ and $rNIR$ denotes diffuse NIR and direct NIR part in the global irradiation. Coefficient k in every equation represents the respective extinction coefficient for the canopy layer. β is the solar elevation angle.

4 Longwave radiation exchange

The net longwave radiation fluxes from surface 1 to surface 2 are described as:

$$QR_{12} = \frac{\varepsilon_1 \varepsilon_2 F_{12} A_1 \sigma}{1-(\rho_1 \rho_2 F_{12} F_{21})}(T_1^4 - T_2^4)$$

Where ε is the surface emissivity, ρ is the surface reflectivity of the longwave radiation, F_{12} is the view factor from surface 1 to surface 2, F_{21} is the view factor from surface 2 to surface 1, σ is the Stefan Boltzmann constant.

5 Air exchange rate

Three different forms of air exchange between the greenhouse and outside environment are implemented in the model, i.e. air leakage from the covering crack and chink of the greenhouse openings, natural ventilation through the greenhouse windows which is driven by the wind and temperature effects, and forced ventilation driven by mechanical fans installs on the side walls of greenhouses.

The leakage accounts for a small and uncontrollable ventilation flux since the greenhouse is not completely air-tight. This leakage flux can be determined using a predetermined value of air exchange rate, which is normally in the range of 0.5-1 [1/h].

The natural ventilation rate is determined using the flowing relation proposed by Boulard and Baille(*4*) for a greenhouse equipped with only a roof or only side openings:

$$Q_{vent} = \frac{A}{2} C_d (2g \frac{\Delta T}{T_0} \frac{H}{4} + C_w u^2)^{0.5}$$

Where C_d is the discharge coefficient, C_w is the wind effect coefficient, ΔT is the temperature difference between the inside and outside air, A is the area of the opening, H is the vertical height of the opening, u is the wind velocity, and g is the gravitational acceleration.

6 Canopy transpiration

Crop transpiration in greenhouses can be estimated based on the mass transfer theory, which links the transpiration to the leaf-to-air vapor pressure deficit, shown as:

$$\lambda_{eva} ET = 2LAI.\frac{\rho C_{air}}{\gamma}(VP_{canopy} - VP_{air})/(r_a + r_{st})$$

Where ET is the transpiration rate, γ is the psychrometric constant, ρ and C_{air} are the density and specific heat capacity of indoor air, VP_{canopy} is the saturated vapor pressure at the canopy temperature, VP_{air} is the partial vapor pressure of the indoor air, r_a and r_{st} are the aerodynamic resistance and stomatal resistance, respectively.

The aerodynamic resistance of the canopy regulates the transfer of water vapor from the leaf surface to the surrounding air, which can be calculated by the classic mass transfer theory based on heat-mass analogy, as we have discussed above. Specifically,

$$r_a = 1/h_{m,canopy-air}$$

Where $h_{m,canopy-air}$ is the mass transfer coefficient between the canopy and indoor air.

Different from common impermeable boundaries, an additional resistance arising from the complex stomatal behavior should be taken into consideration of the transpiration process. The model should describe this complex influence of environmental factors, such as irradiation level, vapor pressure deficit, carbon oxide concentration, on the aperture of the stomata. In this term, the most recommended empirical equations are that proposed by Stanghellini(*5*), shown as:

$$r_{st} = r_{st,\min}.rf(irrdiation).rf(CO2).rf(VPD)$$

$$rf(irradiation) = \frac{R_{can} + C_{can,1}}{R_{can} + C_{can,2}}$$

$$rf(CO2) = 1 + C_{can,3}(\eta_{mg-ppm} C_{co2} - 200)^2$$

$$rf(VPD) = 1 + C_{can,4}(VP_{canopy} - VP_{air})^2$$

Where R_{can} is the global irradiation above the canopy, C_{can} are four empirically determined parameters, η_{mg-ppm} is the conversion factor from mg/m^3 to ppm concentration.

7 Atmospheric radiation

In the radiative energy balance of the surface directly facing the sky, absorbed atmospheric radiation makes a great contribution. The absorption of atmospheric radiation on a horizontal surface comes primarily from those wavelengths outside the atmospheric window. The incident atmospheric radiation can be calculated as:

$$QR_{atm} = \varepsilon_{atm}.T_{ambient}^4$$

Where ε_{atm} is the effective atmospheric emissivity, $T_{ambient}$ is the surrounding ambient temperature. It should be noted that it is a common practice to use $T_{ambient}$ to characterize the atmospheric radiation, since most of the atmospheric radiation comes from the lower hundred meters of the atmosphere where water vapor, carbon oxide and ozone are strongly emitting. Besides, the effective atmospheric emissivity is a lumped concept which ignores the actual spectral distribution of the incident atmospheric irradiation(*6*). In the practical conditions, ε_{atm} is highly affected by the weather conditions, such as ambient humidity and cloud cover. Many empirical equations have been developed to describe the sole effect of humidity on the atmospheric emissivity, namely the emissivity of clear sky. For example, Begger et al.(*7*) mention:

$$\varepsilon_{sky\_clear} = 0.736 + 0.00571 T_{dp} + 3.318 \times 10^{-6} T_{dp}^2$$

Where T_{dp} is the dew point temperature of the ambient air.

The effect of cloud cover is more complicated, considering the varying height of clouds, multiplex constitution of clouds and different types of clouds. One available empirical expression to account for the impact of clouds is written as(*8*):

$$\varepsilon_{sky} = \varepsilon_{sky\_clear} + C(1 - \varepsilon_{sky\_clear})$$

Where C is the cloud cover fraction, defined as $1 - \frac{I}{I_o}$, according to the total global radiation I, acquired from the measured experimental data at the given location, and the total extraterrestrial radiation I_o, calculated from the AM0 solar spectrum.

Crop growth model

The well-structured explanatory model proposed by Vanthoor(*9*) is adopted here to simulate the greenhouse crop growth. This model is based on the buffer theory and can obtain the leaf area index and dry matter to indicate the growth status. Compared with another widely used model TOMGRO(*10*), Vanthoor model are more suitable for investigating the effects of greenhouse environmental factors on the crop growth. More details of the Vanthoor model can be found in (*11*).

Model validation

To validate the accuracy of the proposed model, the simulation results were compared with the measured indoor temperature during the filed test, as shown in Figure S7. It can be seen from the figure that the curve of simulated temperature agrees well with the actual measured one. The maximum absolute deviation between simulated and experimental data for the model boxes were, respectively, indicating the reliability of the simulation model.

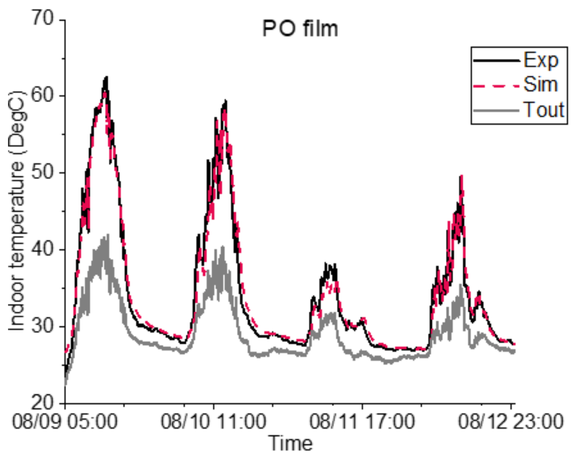

Fig. S7. Comparison of measured and simulated indoor temperature variations in the greenhouse enveloped by PO film

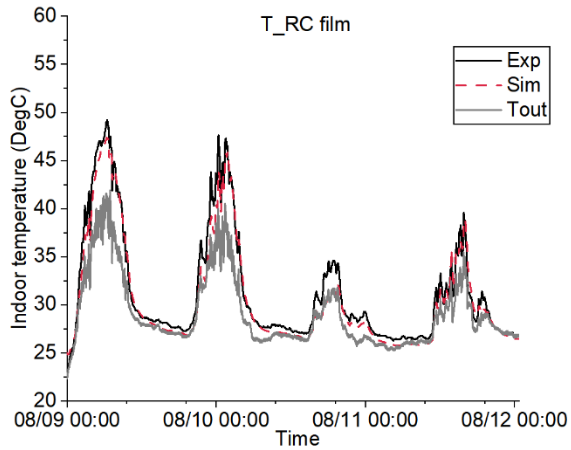

Fig. S8. Comparison of measured and simulated indoor temperature variations in the greenhouse enveloped by T_RC film

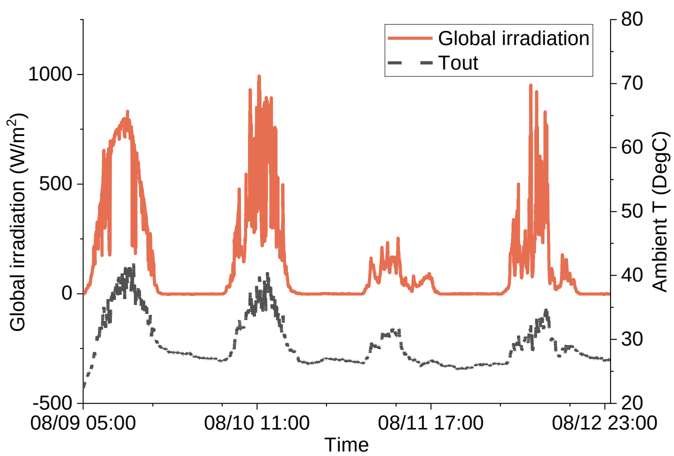

Fig. S9. Measured meteorological data during the experiments

Modeling of the effects of T-RC film on the greenhouse microclimate

Fig.S10a shows the indoor temperature fluctuations inside closed greenhouses during the whole cultivating period of 100 days (starting from 1st April). The peak indoor temperature of the glass greenhouse is 55.87 °C. With the application of T-RC film, the peak indoor temperature can be reduced to 45.56 °C. The maximum temperature drop between the T-RC greenhouse and the glass greenhouse can be up to 10.40 °C (Fig.S10b), indicating the significant cooling effect of the T-RC film. The introduction of ventilation significantly reduces the indoor air temperature, even though the mean cooling effect of T-RC film is also weakened from around 5 °C to 2 °C (Fig.S10c). In the case of greenhouse with shading nets, the cooling effects gradually vanish with the increasing cultivating days.

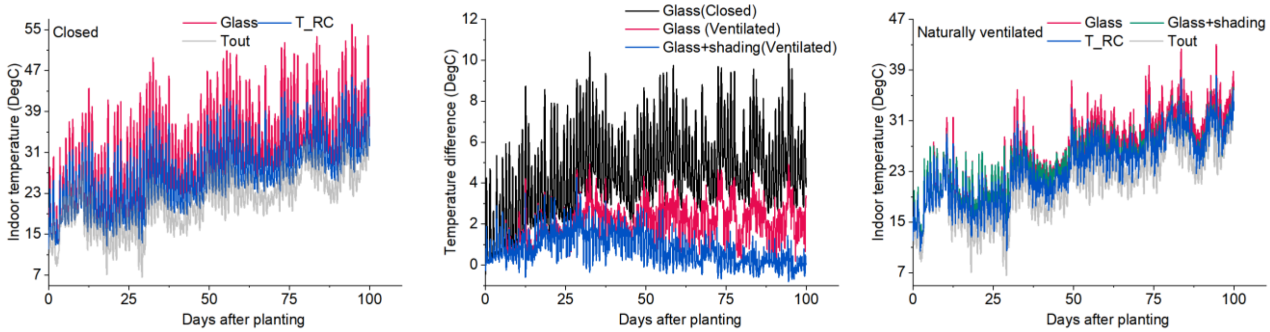

Fig. S10. a. Comparison of indoor air temperature inside closed greenhouses. b. Temperature differences between the T-RC covered greenhouse and conventional glass greenhouses. c. Comparison of indoor air temperature inside naturally ventilated greenhouses.

Reference:

1. Zwart, Analyzing energy-saving options in greenhouse cultivation using a simulation model. *Wageningen, IMAG-DLO rapport, 240 pp. Hfl. 50,00,* (2020).
2. B. H. E. Vanthoor, C. Stanghellini, E. J. van Henten, P. H. B. de Visser, A methodology for model-based greenhouse design: Part 1, a greenhouse climate model for a broad range of designs and climates. *Biosyst. Eng.* **110**, 363-377 (2011).
3. J. C. Roy, T. Boulard, C. Kittas, S. Wang, PA—Precision Agriculture: Convective and Ventilation Transfers in Greenhouses, Part 1: the Greenhouse considered as a Perfectly Stirred Tank. *Biosyst. Eng.* **83**, 1-20 (2002).
4. T. Boulard, A. Baille, J. Lagier, M. Mermier, E. J. J. o. A. E. R. Vanderschmitt, Water vapour transfer in a plastic house equipped with a dehumidification heat pump. **44**, 191-204 (1989).
5. C. Stanghellini, Transpiration of Greenhouse Crops – an Aid to Climate Management. *Prof.dr.ir. J. Schenk (promotor), dr.ir. G.P.A. Bot (co-promotor). Wageningen (1987) 150 pp.,* (1987).
6. D. Zhao *et al.*, Radiative sky cooling: Fundamental principles, materials, and applications. *Applied Physics Reviews* **6**, 021306 (2019).
7. X. Berger, D. Buriot, F. Garnier, About the equivalent radiative temperature for clear skies. *Solar Energy* **32**, 725-733 (1984).
8. M. Martin, P. Berdahl, Characteristics of infrared sky radiation in the United States. *Solar Energy* **33**, 321-336 (1984).
9. B. H. E. Vanthoor, P. H. B. de Visser, C. Stanghellini, E. J. van Henten, A methodology for model-based greenhouse design: Part 2, description and validation of a tomato yield model. *Biosyst. Eng.* **110**, 378-395 (2011).
10. J. W. Jones, E. Dayan, L. H. Allen, Keulen, H. Challa, A dynamic tomato growth and yield model (TOMGRO). *Transactions of the ASAE* **34**, (1991).
11. B. Vanthoor, A model-based greenhouse design method. Wageningen: Wageningen Agricultural University (2011).